Article

Interaction of Ethanol with Biological Membranes: The Formation of Non-bilayer Structures within the Membrane Interior and their Significance

Andrey A. Gurtovenko, and Jamshed Anwar

More About This Article

Additional resources and features associated with this article are available within the HTML version:

- Supporting Information
- Access to high resolution figures
- Links to articles and content related to this article
- Copyright permission to reproduce figures and/or text from this article

View the Full Text HTML

Interaction of Ethanol with Biological Membranes: The Formation of Non-bilayer Structures within the Membrane Interior and their Significance

Andrey A. Gurtovenko and Jamshed Anwar*

Computational Biophysics Laboratory, Institute of Pharmaceutical Innovation, University of Bradford, Bradford, West Yorkshire, BD7 1DP, United Kingdom

Received: September 10, 2008; Revised Manuscript Received: November 13, 2008

To gain a better understanding of how ethanol affects biological membranes, we have performed a series of atomic-scale molecular dynamics simulations of phospholipid membranes in aqueous solution with ethanol, whose concentration was varied from 2.5 to 30 mol % (lipid-free basis). At concentrations below the threshold value of ~12 mol % (30.5 v/v %) ethanol induces expansion of the membrane, accompanied by a drop in the membrane thickness as well as disordering and enhanced interdigitation of lipid acyl chains. These changes become more pronounced with increase in ethanol concentration, but the bilayer structure of the membrane is maintained. Above the threshold concentration the appearance of multiple transient defects in the lipid/water interface eventually gives rise to desorption and assembly of some of the lipids into non-bilayer structures within the membrane interior. These structures, being small and irregular, resemble inverted micelles and have a long-lived character. Furthermore, formation of the non-bilayer structures is accompanied by mixing of lipids that belong to the opposite membrane leaflets, thereby leading to irreversible changes in the membrane structure. Remarkably, this observation of the formation of non-bilayer structures within the membrane interior, being in good agreement with experimental data, is found to be robust with respect to both the simulation conditions (the system size and the presence of salt) and the type of lipids (phosphatidylcholine and phosphatidylethanolamine). We discuss the significance of these non-bilayer structures in relation with the well-known ability of ethanol to promote membrane hemifusion as well as with the possible role of the micelle-like structures as a delivery system for polar solutes and ions. The ethanol-induced "damage" to the bilayer structure also suggests that strong alcoholic beverages (~40 v/v %) might be potentially hazardous to the epithelial tissues of the human body (such as lips, mouth, throat, gullet, and stomach) that come in direct contact with high-concentrations of ethanol.

Introduction

The modulation of the properties and function of plasma membranes by small amphiphilic solutes is important for many biomedical applications, including anesthesia, cryopreservation and permeation enhancement. Ethanol, being a short chain alcohol, is a particularly important representative of molecules that can modulate properties of membranes. Apart from the fact that it is widely consumed as a principal component of alcoholic beverages, ethanol has important applications as a food preservative, a permeability enhancer in transdermal drug delivery, and as a model anesthetic. How ethanol interacts with lipid membranes is fundamental to each of these applications. This interaction is also of fundamental biophysical interest as ethanol can modulate the phase stability of lipids and can induce the formation of interdigitated bilayer structures.

A key issue of physiological relevance in connection with exposure of tissues to ethanol is that of adaptive change in membranes when exposed to ethanol, leading to tolerance on subsequent exposure. Although ethanol-induced adaptation is thought to involve changes in lipid metabolism and interactions with proteins, the picture is far from clear, and a physical basis cannot be discounted.[1] Repeated exposure to ethanol may selectively alter the composition of lipids conferring resistance to ethanol upon subsequent exposure. The ability of ethanol to enhance membrane permeability is exploited in transdermal drug delivery, where ethanol is a common component of topical formulations.[2] The understanding of how ethanol exerts this effect, particularly at a molecular level, is still lacking. Notably, its penetration-enhancing capability appears to be concentration dependent, and studies have reported that high concentrations of ethanol can retard drug permeation.[3] The mechanism of action of anesthetics including ethanol is still not entirely resolved. A number of studies suggest that anesthetics directly influence membrane proteins and can block, for example, ionic channels, thereby inhibiting cellular signaling.[4] The problem with this site-specific hypothesis is that ethanol is known to affect many different proteins across different tissues and cell types, and effective concentrations are typically higher than those expected for a receptor-type interaction. The alternative mechanism that appears to be gaining momentum is that of "indirect" action where the anesthetic molecules affect membrane proteins indirectly by modulating the properties of the lipid membrane.[5]

Given the significance of the interaction of ethanol with lipid membranes, it is not surprising that this area has been the focus of numerous experimental and computational studies. These studies are beginning to reveal a molecular level picture of how ethanol can modulate the structural and mechanical properties of membranes. Although ethanol has an amphiphilic character, being a short-chain alcohol, its hydrophobicity is limited. Therefore, after partitioning into a lipid membrane, ethanol molecules are primarily located within the water/lipid interface,

---

* To whom correspondence should be addressed. E-mail: j.anwar@bradford.ac.uk.

TABLE 1: Summary of MD Simulations of POPC Membranes with Ethanol

system	C_{Eth} [mol %][a]	C_{Eth} [v/v %][a]	ethanol/lipid molar ratio	<A> [nm^2][b]	P–P distance [nm][c]	⟨α⟩ [°][d]
1	0.0	0.0		0.65 ± 0.01	3.83 ± 0.06	77.9 ± 1.3
2	2.5	7.6	1.6:1	0.77 ± 0.01	3.48 ± 0.04	79.8 ± 1.5
3	5.0	14.6	3.2:1	0.91 ± 0.01	3.18 ± 0.04	79.8 ± 1.7
4	10.0	26.2	6.3:1	1.09 ± 0.03	2.92 ± 0.05	80.1 ± 1.9
5	15.0	36.2	9.5:1			
6	30.0	58.0	18.8:1			

[a] Molar and volume/volume concentrations of ethanol in the system. [b] The area per lipid, <A>; error margins throughout the study were computed as standard deviations. [c] The thickness of a membrane defined as the distance between the average positions of phosphorus atoms on two sides of the membrane. [d] The average angle between the P–N vector of a lipid headgroup and the outward bilayer normal.

forming hydrogen bonds with hydrophilic lipid head groups.[6,7] The presence of ethanol in the membrane has a disordering effect on lipid hydrocarbon chains, giving rise to an increase in the area per lipid and the overall fluidity of the membrane.[8,9] This is accompanied by a drop in the membrane thickness and by a reduction in the tension at the membrane/water interface and in the membrane rigidity.[10,11] Recent molecular dynamics simulation studies have addressed the problem of the effect of ethanol on the structure of lipid membranes,[12,13] membrane dynamics,[14,15] and the lateral pressure profile within a bilayer.[15] The lateral pressure differential across a bilayer is considered to be the means by which perturbing molecules transmit their effect onto protein structures embedded in the membrane, thereby inducing a structural change within the protein.[15] Simulations have also been employed to ascertain how a variation in the chain length of alcohol molecules can influence the structure and properties of model bilayers.[16,17]

Most of the above studies, in particular the simulation studies that are able to provide the molecular-level resolution, have been limited to specific, relatively low concentrations of ethanol. We now take the next step and systematically explore the sensitivity of model lipid membranes to a wide range of ethanol concentrations in a bid to address issues such as whether ethanol can induce water pores, as has been observed for the small molecule dimethylsulfoxide,[18,19] and the possible mechanism of action of ethanol in inducing hemifusion between protein-free bilayers.[20] Toward this end we performed a series of atomic-scale molecular dynamics (MD) simulations of phosphatidylcholine membranes under the influence of ethanol concentrations of up to 30 mol % and also examined the influence of monovalent ions (Na$^+$, K$^+$, and Cl$^-$) on the ethanol–lipid interaction. We demonstrate that there is a certain threshold concentration of ethanol above which some of the lipid molecules become involved in forming non-bilayer, reverse micelle-like structures within the interior of the initial membrane. These structures could serve as "transport delivery systems" for polar solutes and also explain the role of ethanol as a desorbing agent in hemifusion.

Methods

Atomic-scale molecular dynamics simulations were carried out for single-component lipid bilayers comprised of zwitterionic palmitoyl-oleoyl-phosphatidylcholine (POPC) lipids in aqueous solution with ethanol. A typical simulation system consisted of 128 POPC lipids and ~8000 solvent molecules (water and ethanol). The concentration of ethanol was systematically varied from 2.5 to 30 mol %, the specific concentrations being 2.5, 5.0, 10.0, 15.0, and 30.0% (lipid-free basis), see Table 1. The total number of atoms in the bilayer systems varied from 30 700 to 33 000, depending on ethanol concentration.

Force-field parameters for POPC lipids were taken from the united atom force-field of Berger et al.[21] Water was modeled using the simple point charge (SPC) model.[22] For ethanol the GROMOS87 set of parameters implemented in the GROMACS simulation suite was used.[23] The Lennard–Jones interactions were cut off at 1 nm. For the electrostatic interactions, we used the particle-mesh Ewald method.[24,25] Simulations were performed using the GROMACS suite[23] in the NpT ensemble with semi-isotropic pressure coupling, where the simulation box in the direction of the bilayer normal (z-axis) and the cross-sectional area of the box in the x–y plane could vary independently. The temperature (set to $T = 310$ K) was kept constant using a Berendsen thermostat[26] with a coupling time constant of 0.1 ps. Pressure (set to 1 bar) was controlled by a Berendsen barostat[26] with a coupling time constant of 1.0 ps. The time step used in the simulations was 2 fs. All lipid/water/ethanol systems listed in Table 1 were simulated for 100 ns each. As a reference, a 100 ns long MD trajectory of an ethanol-free POPC lipid bilayer was taken from refs 27 and 28.

At 15 mol % of ethanol we observed a remarkable event of formation of non-bilayer structures within the membrane. In view of this, we performed several additional simulations at this ethanol concentration to elucidate the sensitivity of this observation to solvent/lipid ratio, system size, a different type of lipid, and to the inclusion of monovalent ions. These simulations included (i) a 25 ns long MD run of a POPC bilayer system in which the number of solvent molecules (water and ethanol) was increased by a factor of 1.5; (ii) a 20 ns long MD run of a POPC bilayer system whose size was doubled with respect to the original system; (iii) a 30 ns long MD run of a bilayer system in which POPC lipids were replaced by palmitoyl-oleoyl-phosphotidylethanolamine (POPE) lipids, the PE head groups being described following the POPE model of Tieleman and Berendsen;[29] and (iv) two 100 ns long MD simulation runs of POPC/ethanol/water systems with added NaCl or KCl salt, with the salt concentration being set to ~0.25 M, that is, not far from the physiological values. For sodium and chloride ions we used the force-field parameters developed in ref 30 and supplied with the GROMACS force-field.[23] For potassium ions the parameters developed by Roux and Beglov[31] were employed. These force-field parameters for Na, K, and Cl ions were successfully used in a recent study of salt-induced effects on phospholipid membranes.[28] Furthermore, to identify more precisely the threshold ethanol concentration at which the formation of the non-bilayer structures occurs, we performed a series of simulation runs (30–50 ns long) of POPC bilayer systems with 11, 12, 13, and 14 mol % of ethanol.

To get an indication of the lifetime of the ethanol-induced micellular structures that formed within the membranes, we performed a series of 5 short subsequent runs (5 ns each) on the bilayer system containing an initial concentration of ethanol

Interaction of Ethanol with Biological Membranes

J. Phys. Chem. B, Vol. 113, No. 7, 2009 **1985**

of 15 mol % from which all ethanol molecules were removed from the water phase and the lipid/water interface. These simulations aimed to explore whether the bilayer structure of a membrane could be recovered by a stepwise reduction in the ethanol concentration.

Finally, the above simulations were complemented by two 90 ns long MD runs of a mixture of POPC lipid, ethanol, and water at ethanol concentrations of 15 and 30 mol % (lipid-free basis) starting from a random configuration to look at the self-assembly of these components. The overall simulated time in the entire study exceeded 1.1 microseconds.

For the analysis the area per lipid was considered as a key parameter for identifying equilibration. On this basis it was found that all systems for which the bilayer structure was maintained equilibrated within 30 ns. Consequently, only the last 70 ns of the 100 ns trajectories were used for the analysis.

Results

A. Moderate Concentration of Ethanol. We start with a discussion of the effects of moderate concentrations of ethanol, namely 2.5, 5.0, and 10.0 mol %, on POPC lipid membranes.

Before studying ethanol effects, we validate the lipid bilayer model employed in this study. A fundamental characteristic for comparison with experiment is the average area per lipid, which defines to a large extent other structural and dynamical characteristics such as the membrane thickness, the ordering of lipid acyl chains, and the lateral diffusion of lipids. For the ethanol-free POPC bilayer at $T = 310$ K the area per lipid was found to be 0.65 ± 0.01 nm^2 (see Table 1), which is close to the reported experimental values of 0.66 nm^2 ($T = 310$ K),[32] 0.65 nm^2 ($T = 298$ K),[33] 0.64 nm^2 ($T = 298$ K),[34] and 0.63 nm^2 ($T = 297$ K),[35] and also to the values obtained in earlier atomistic simulation studies, 0.655 nm^2 ($T = 300$ K),[36] 0.62 nm^2 ($T = 298$ K),[37] and 0.66 nm^2 ($T = 310$ K).[38] Clearly, the molecular model employed provides a reasonable description of a POPC lipid bilayer at physiological temperature.

As evident from Table 1, adding ethanol molecules to a lipid bilayer has a dramatic effect on the membrane structure. In particular, one can witness a considerable expansion of the membrane (by up to 70% at 10.0 mol % of ethanol), which is accompanied by a drop in the membrane thickness. These findings are in agreement with experimental data[8−11] and results of existing atomic-scale simulation studies.[12,13,16,17,39] An increase in the area per lipid is normally a signature of an enhanced fluidity of a lipid membrane, implying a more disordered hydrophobic membrane core. Indeed, this can easily be seen from the calculated deuterium order parameter S_{CD} of the hydrocarbon lipid chains, see Figure 1.

The order parameter S_{CD} is defined separately for each hydrocarbon group as $S_{CD} = 3/2 \langle \cos^2 \theta \rangle - 1/2$, where θ is the angle between a CD-bond and the bilayer normal. Since a united-atom force field is employed, the positions of the deuterium atoms are not directly available but can be reconstructed from the coordinates of three successive nonpolar hydrocarbons under assumption of an ideal tetrahedral geometry of the central hydrocarbon group.[40,41] In practice, we calculated S_{CD} with the use of the routine "g_order" supplied with the Gromacs suite.[23] The effect of ethanol on the ordering of the upper part of acyl chains (first 6 S_{CD} groups from the glycerol group) turns out to be non-monotonic: rather small concentrations of ethanol (2.5 mol %) lead to a slight enhancement of the order, whereas further increase in ethanol concentration gives rise to a pronounced disordering of hydrocarbon lipid chains, including their upper parts (Figure 1). This finding is in full
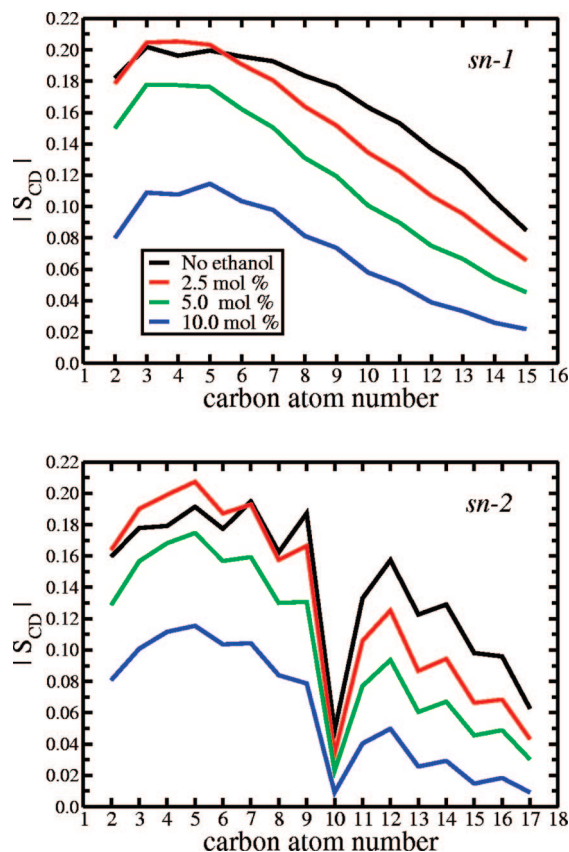

Figure 1. Deuterium order parameter $|S_{CD}|$ for saturated *sn*−1 (top) and unsaturated *sn*−2 (bottom) acyl chains of POPC lipids at different concentrations of ethanol. Low carbon atom numbers correspond to those close to the headgroup.

agreement with the results of ref 12 and reflects the competition of two opposing factors: membrane expansion and hydrogen bonding of ethanol molecules to lipid head groups.[16] The former promotes disordering of lipid chains, and the latter locally enhances chain order, especially in the region adjacent to the head groups. However, at higher ethanol concentrations (≥ 5.0 mol %) the first factor dominates, and one can clearly see a dramatic ethanol-induced disordering of the lipid acyl chains.

The preferred location of ethanol molecules is revealed by the component-wise mass density profiles of the bilayer systems in question. In Figure 2 we present these density profiles for the four POPC bilayers in aqueous solution with 0, 2.5, 5.0, and 10.0 mol % of ethanol. First of all, it is seen that for all the bilayer systems the peaks in the ethanol mass density (i.e., the preferred locations of ethanol molecules) are just beneath the phosphate groups of the lipids. The peaks do not disappear even at a rather high ethanol concentration (10 mol %), suggesting strong (hydrogen-bond mediated) interactions between lipid head groups and ethanol molecules.[16] At the low concentrations of 2.5 and 5.0 mol % the probability of finding ethanol within the hydrophobic core of the membrane (i.e., close to $z = 0$ in Figure 2) is very small but begins to increase at the higher concentration of 10 mol %. To illustrate the location of ethanol within the membranes, we present snapshots of the POPC bilayer with ethanol (5 mol %) and without ethanol in Figure 3.

Ethanol drastically changes the shape of the density profile of POPC lipids. The two main peaks corresponding to the region of lipid head groups get smaller, while at the same time the density of the hydrocarbon chains in the middle of the membrane increases. As a result, the density profile typical of PC lipid
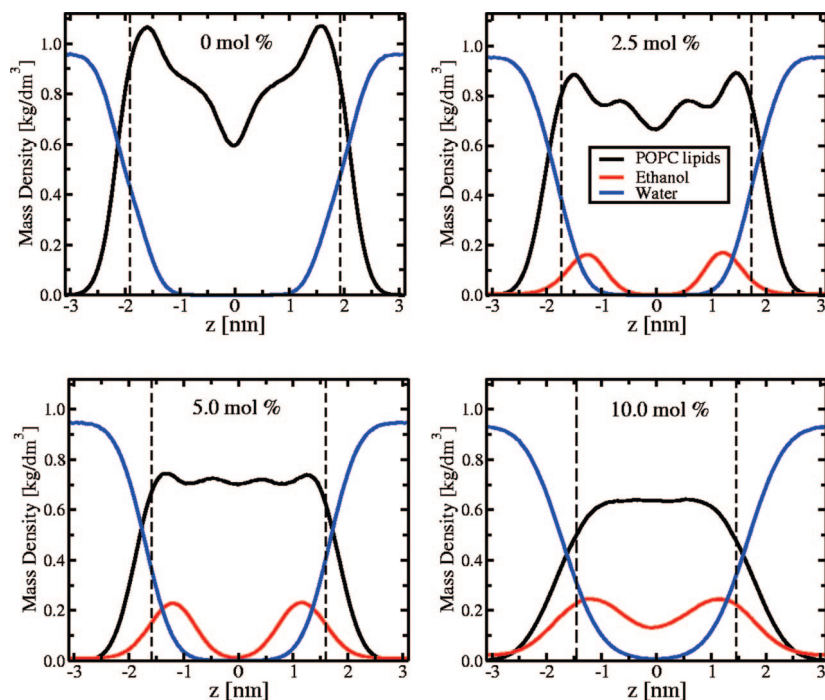
Figure 2. Component-wise mass density profiles for POPC bilayer systems with 0, 2.5, 5.0, and 10.0 mol % of ethanol. Shown are density profiles for POPC lipids (black lines), ethanol molecules (red lines), and water (blue lines). The average positions of phosphorus atoms of lipid head groups (indicating the membrane thickness) are shown by vertical dashed lines.

bilayers gradually transforms with increasing ethanol concentration, reaching a plateau at 10 mol % of ethanol, see Figure 2. We note that similar effects were also reported in ref 16, but the authors did not observe the density plateau, presumably because the ethanol/lipid molar ratio studied (2.2:1) was considerably lower compared to that in our study (6.3:1).

The above-mentioned increase in the density in the middle of the membrane, being coupled to a significant drop in the membrane thickness, suggests that the lipid chains are interdigitated, that is, hydrocarbon chains of one membrane leaflet can be found in the region that is normally occupied by the chains of the opposite leaflet. In Figure 4 we present density profiles of lipid molecules calculated separately for the two leaflets, the area of their overlap therefore being a measure of chain interdigitation. It is apparent that the acyl chains of a POPC bilayer in the fluid phase are interdigitated to some extent even without ethanol. However, ethanol further enhances this interdigitation, the effect being concentration-dependent and most pronounced at the highest concentration (10 mol %), see Figure 4. These computational results are consistent with experimental observations of ethanol-induced interdigitation of acyl chains of unilamellar DPPC bilayers.[42]

Of particular interest is the orientation of lipid head groups with respect to the outward bilayer normal, as the headgroup tilt is crucial for the electrostatic properties of lipid bilayers.[28] The average values for the tilt of the lipid head groups are presented in Table 1 for different concentrations of ethanol. Surprisingly, the tilt angle stays almost unchanged under the presence of ethanol, demonstrating only a very slight increase (by ∼2°). Inspection of corresponding distributions of the angle between the P–N headgroup vector and the outward bilayer normal shows a slight widening of the distribution toward the region of large angle values, indicating an increase in the fraction of lipids whose head groups point to the membrane interior. The relative insensitivity of the headgroup tilt to ethanol was also reported in earlier simulations.[12] Such a behavior is rather

counter-intuitive: membrane expansion due to insertion of ethanol molecules into the lipid/water interface should lead to an increase of the lateral distance between neighboring lipids and, as a result, to the reorientation of the lipid headgroups toward the water phase due to breakage of charge pairing between the phosphate and choline groups.[43] This effect was indeed observed in a recent study of phospholipid membranes under the influence of dimethyl sulfoxide (DMSO), another small amphiphilic solute.[18,19] In the case of ethanol, it is likely that the reorientation of headgroups due to membrane expansion is compensated by strong hydrogen bonding of ethanol with lipids.

Ethanol, therefore, has a pronounced effect on the structural properties of phospholipid membranes, and being amphiphilic in nature it can easily partition into the lipid/water interface and in so doing induces a marked expansion of the membrane. We note here that these changes are concentration-dependent and appear to be reversible, as the bilayer structure of membranes is preserved at moderate concentrations of ethanol (≤10 mol %). As we will see below, further increase in ethanol concentration can damage phospholipid bilayers in an irreversible manner.

B. High Concentration of Ethanol. When the concentration of ethanol in the bilayer system increases to 15 mol % and beyond, the character of ethanol-induced changes becomes markedly different. These induced changes are visualized in Figure 6 for a POPC membrane with 15 mol % of ethanol. In the early stages of the simulation, the effect of ethanol is similar to that observed at lower ethanol concentrations: the membrane expands, accompanied by a drop in its thickness. However, at some point the progressive thinning of the membrane, along with increased hydrophilicity of the membrane interior due to accumulation of ethanol molecules, makes the lipid/water interface unstable and prone to formation of defects. As a result, one can observe the appearance of several "water fingers" in the interior of the membranes that are lined with lipid head

Interaction of Ethanol with Biological Membranes

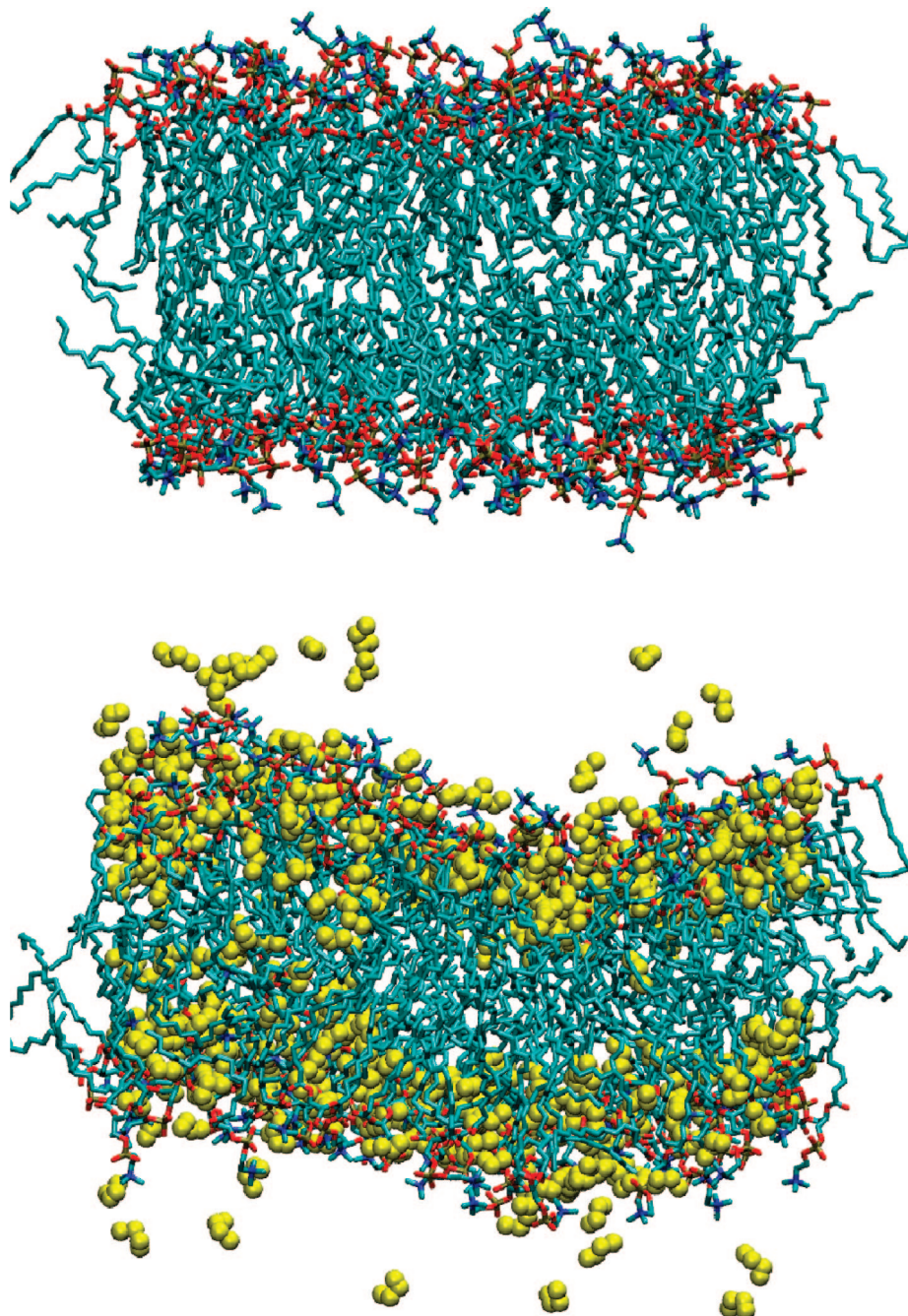*J. Phys. Chem. B, Vol. 113, No. 7, 2009* **1987**

Figure 3. Snapshots of final structures (after 100 ns of simulations) of POPC bilayers without ethanol (top) and with 5.0 mol % of ethanol (bottom). Lipids are shown in cyan and ethanol molecules in yellow; water is not shown.

groups, see snapshot 2 in Figure 6. This picture is akin to that seen in simulations of phospholipid bilayers with dimethyl sulfoxide (DMSO).[18,19] However, there is an important difference: the water defects from the opposite leaflets do not meet each other inside the membrane, so that formation of a water pore, as observed for DMSO, does not occur in the lipid bilayers under the influence of ethanol. A possible reason for this might be that strong interactions (hydrogen bonds) between ethanol molecules and the lipid head groups, which (in contrast to DMSO molecules) can considerably reduce headgroup hydrophilicity and effectively screen the lipid head groups from their counterparts in the opposite leaflet. Instead of pore formation, one can witness "desorption" of a cluster of water molecules surrounded by head groups toward the membrane interior, see snapshot 3 in Figure 6. In fact, this implies that the bilayer structure of the membrane becomes partly destroyed: in the

membrane interior one can now see several non-bilayer globular structures that have the form of irregular "inverse micelles" (snapshot 4 in Figure 6).

We note that we were not able to equilibrate bilayer systems with 15 and 30 mol % within a 100 ns simulation run. The area of a membrane had its maximal value at the point of initial formation of the non-bilayer structures in the membrane interior and then gradually decreased as more and more lipid molecules desorbed from the lipid/water interface toward the interior. This process is also accompanied by an increase of an "effective" membrane thickness (cf. snapshots 3 and 4 in Figure 6). In part, such a progressive compression of a membrane is due to the semi-isotropic type of pressure coupling employed (the size of a simulation box in the direction of the bilayer normal (z-axis) and the cross-sectional (x–y) area of a bilayer were varied independently). The desorption of some of the lipids from the
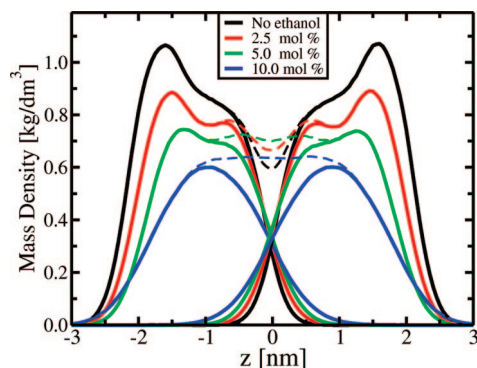
Figure 4. Highlighting interdigitation: component-wise mass density profiles for the opposite leaflets of POPC bilayers without ethanol (black lines) and with 2.5 (red lines), 5.0 (green lines), and 10.0 mol % (blue lines) of ethanol. The density profiles of all lipids in the membranes are shown by dashed lines.
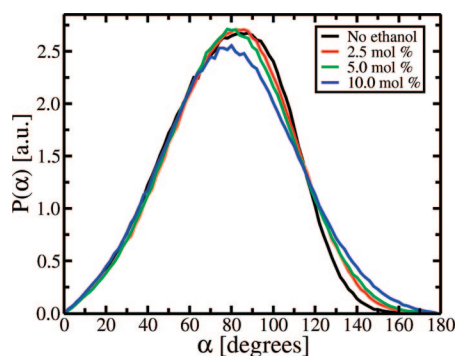

Figure 5. The distribution $P(\alpha)$ (in arbitrary units) of the angle α between P − N vectors of POPC headgroups and the outward bilayer normal for different concentrations of ethanol.

bilayer causes a pressure drop in the $x-y$ direction, which drives the membrane compression process. The compression itself probably facilitates further transfer of the lipids into the membrane interior, as the resulting stress would be easily accommodated in the independent z-direction. When the pressure coupling was switched to an isotropic type, the membrane compression stopped. To confirm that the formation of the non-bilayer "micelle-type" structures was not an artifact of the pressure coupling, we carried out simulations of the self-assembly of a lipid/ethanol/water system containing 15 and 30 mol % of ethanol (lipid-free basis) and demonstrated that a part of the lipid molecules ended up being organized in inverse micelle-type structures.

To further visualize the structure of a POPC membrane under the influence of a high concentration of ethanol, we present a snapshot and component-wise density profiles for the bilayer system with 15 mol % of ethanol in the middle of a 100 ns simulation run in Figure 7. First of all, it is seen that the lipid/bilayer interface is preserved (at $z \cong 3$ nm and $z \cong 10$ nm). A small fraction of water molecules is trapped in the membrane interior; at the same time, the density profiles for choline and phosphate groups appear inside the membrane in a rather structured manner, which is a sign of formation of small micelle-like structures in the hydrophobic core of the membrane, see Figure 7. Interestingly, these non-bilayer structures can serve as traps not only for water molecules but also for salt ions: the simulations of systems containing NaCl and KCl salt reveal similar micelle-like structures in the membrane interior but now containing individual ions, see Figure 8. The ion-containing micellular structures remain in the membrane interior throughout the simulations. One could hypothesize that the micelle-like

structures could play the role of carriers for hydrophilic solutes in transporting them from one side of the membrane to another, although we did not observe such a transport event in the bilayer systems within the various 100 ns simulation runs.

We examined the sensitivity of the micelle-formation phenomenon to system size by performing two additional simulations of the bilayers with 15 mol % of ethanol, in which we either increased the number of solvent molecules (water and ethanol) by a factor of 1.5 or doubled the overall size of the system. These systems revealed a similar behavior to the reference system. It should be noted, however, that this doubling of the size of the bilayer patch is probably still not sufficient to fully elucidate possible system size artifacts. For instance, increasing the size of the system by a factor of about 10 is likely to promote thermally driven undulatory motion of the lipid bilayer, which will probably facilitate ethanol-induced desorption of lipid molecules into the bilayer interior. We also investigated whether micelle formation in the membrane interior would occur for another lipid type and proceeded to replace POPC with palmitoyl-oleoyl-phosphatidylethanolamine (POPE). Remarkably, the POPE membrane also showed desorption of lipids and subsequent formation of micelles in the membrane interior. We recall that a POPE lipid has a primary amine in the headgroup (instead of a choline group in POPC), and therefore POPE lipids are capable of forming intra- and intermolecular hydrogen bonds.[44] As a result, the water−lipid interface of a POPE bilayer is considerably more densely packed as compared to a POPC bilayer.[28] The fact that the effect of high concentration of ethanol on POPC and POPE membranes was found to be similar would suggest that this effect may be of a generic nature.

We explored the reversibility of the changes induced by high concentrations of ethanol. First, we manually "washed" the membrane shown in Figure 7 (top) by removing all ethanol molecules from the water phase and from the outer part of the lipid/water interface. The resulting system was then simulated for 5 ns. This procedure was repeated 5 times, after which the overall concentration of ethanol in the bilayer system dropped from 15 mol % to 7.8 mol %. However, a test 10 ns long simulation of the final system showed no changes in non-bilayer structures inside the membrane. Visual inspection of the resulting system suggests that the non-bilayer micelle-like structures within the membrane were stabilized to some extent by the reduction in ethanol concentration. Namely, the acyl chain regions around the micelles (see e.g. Figure 7 (top)) restore their hydrophobicity due to the drop in ethanol concentration. As a result, the recovery of the original bilayer structure is now energetically unfavorable because it implies contacts of lipid head groups trapped in micelles with hydrocarbon chains. Therefore, one can conclude that the changes induced by high concentrations of ethanol in the lipid membranes are most likely to be long-lived, certainly in terms of the nanosecond time scale accessible to simulation. An estimation of their life-times is not feasible due to time-scale limitations of MD simulations. What is more, we observed that lipids involved in the micelle-like structures belong to both leaflets, so that one can witness an extensive mixing of lipids from the opposite leaflets of the original bilayer. Thus, even if the original bilayer structure is recovered with time, its lipid composition will be completely different. In the light of this, the lipid membrane changes induced by high concentrations of ethanol can be considered to be irreversible.

Can the rather remarkable observation that ethanol-induced formation of micelle structures in the membrane interior as observed in the simulations be linked with experimental data?
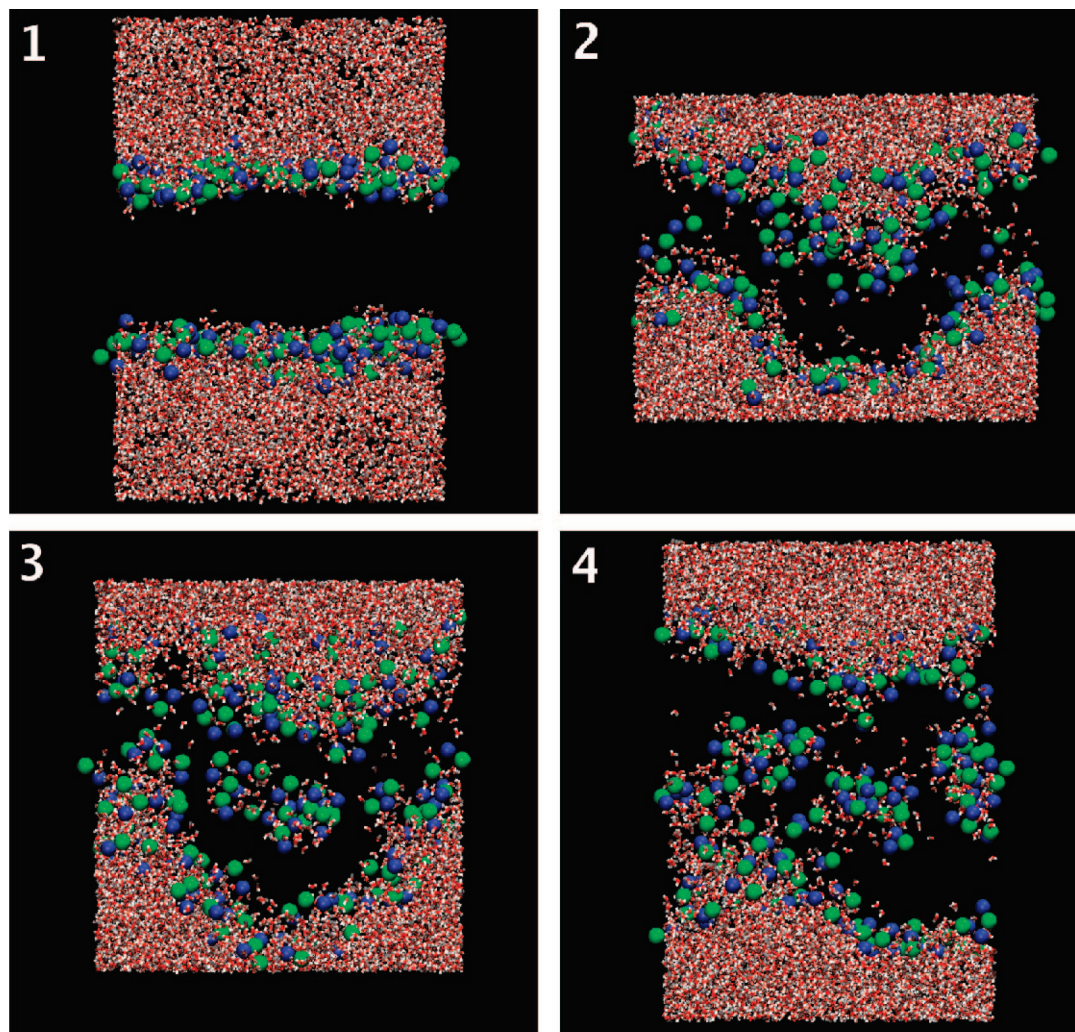
Interaction of Ethanol with Biological Membranes

J. Phys. Chem. B, Vol. 113, No. 7, 2009 **1989**

Figure 6. Formation of non-bilayer structures within the membrane interior for the POPC system with 15 mol % of ethanol: (1) 3100 ps; (2) 13 180 ps; (3) 19 920 ps; (4) 30 000 ps. Shown are water molecules (red and white) and phosphorus (green) and nitrogen (blue) atoms of lipid headgroups. The rest of the lipid atoms as well as ethanol molecules are not shown.

The answer here is yes, although the correspondence is not exact. It has been observed experimentally that ethanol concentrations exceeding 29.4 v/v % (11.5 mol %) cause a transformation of the bilayer structure of DPPC membranes to small globules.[42] The structure of these globules, however, could not be determined due to the limited resolution of the AFM technique employed. Furthermore, Isomaa et al.[45] have demonstrated that small amphiphilic compounds are able to alter the shape of membranes of human erythrocytes and to induce a rapid formation of non-bilayer phases within the interior of the membrane, thereby protecting the membrane against collapse. Interestingly, these changes were found to be relatively long-lived: erythrocytes treated with amphiphiles did not recover their normal shape after washing and reincubation in amphiphile-free solution for up to 1 h.[45] Hence, the simulations, particularly those that explored self-assembly, are clearly in agreement with experiment in that ethanol at high concentrations indeed induces the micelle-type phase.

Upon identifying the link with experiment we proceeded to titrate the ethanol concentration to see whether it is possible to get a closer match with experimental data in terms of the critical ethanol concentration that induces formation of micelle structures in the interior of the membrane. A series of relatively short (30−50 ns long) simulations were performed on a POPC bilayer system with ethanol concentrations in the range between 10 mol % (at which the bilayer structure is preserved) and 15 mol % (where partial loss of the bilayer structure occurs). It turns out that the formation of non-bilayer structures within the membrane is first observed at an ethanol concentration equal to 12 mol %, which agrees very well with the experimentally observed value of 11.5 mol %. [42]

Discussion

The main finding of this study is the formation of non-bilayer, micelle-like structures within the membrane interior under the influence of high concentrations of ethanol (>12 mol %). To the best of our knowledge this is the first report of such a phenomenon revealed by atomic-scale MD simulations. As such, the idea of non-bilayer structures is not new and indeed has been proposed by experimentalists to explain structural changes induced by small amphiphillic molecules in membranes.[42,45]

Our results also shed some light on the experimentally observed ability of ethanol to promote membrane hemifusion (the linking of two leaflets of two adjacent membranes before the formation of a fusion pore).[20] The key determinants of hemifusion promoters appear to be their ability to reduce the bending rigidity of the membranes and to support a negative curvature of the emerging stalk during the hemifusion process. Ethanol certainly reduces the bending rigidity, which is readily
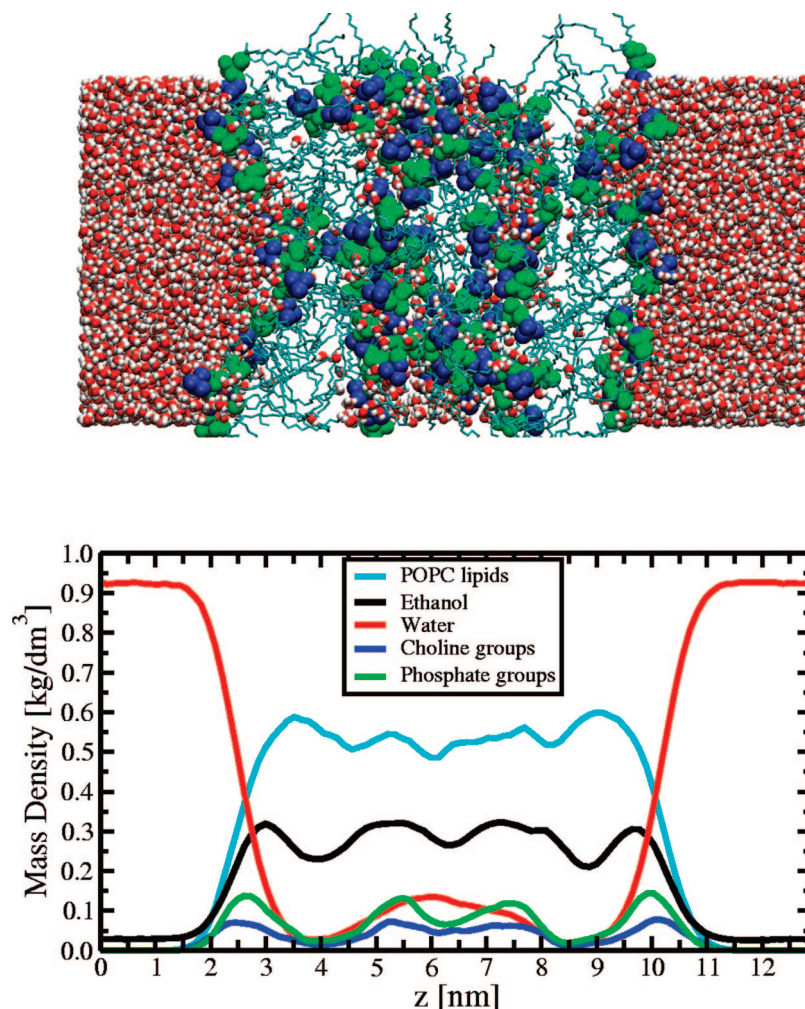
Figure 7. (Top) The structure of a POPC membrane in aqueous solution with 15 mol % of ethanol after 50 ns of simulations. Lipid acyl chains are shown in cyan, phosphate groups of lipids in green, choline groups in blue, and water in red and white. Ethanol molecules are not shown. (Bottom) Corresponding component-wise mass density profiles calculated for the part of the MD trajectory from 40 to 50 ns. Shown are density profiles for POPC lipids (cyan line), ethanol molecules (black lines), water (red lines), choline (blue), and phosphate (green) groups of lipid head groups.

apparent in the simulations from the tendency of the bilayers to show thermal undulations with increasing ethanol concentration but is apparently considered to have a positive spontaneous curvature.[46,47] In view of this, ethanol's primary mode of action in promoting hemifusion has been considered to be its ability to cause transient breakage in the two adjacent lipid leaflets so as to enable the subsequent merger that gives rise to stalk formation. This translates to a decrease in the tensile strength of the lipid membrane. The formation of the micelle-like structures as observed in our simulations also involves transient breakage in the individual bilayer leaflets. As the formation of the micelle structures appears to be a generic effect, it is clear that ethanol does indeed readily enable the desorption and/or breakage of lipids from the leaflets as proposed by Chanturiya et al.[20]

From a physics perspective it is important to rationalize why ethanol does not form water pores as observed for DMSO. DMSO molecules prefer to reside just below the lipid headgroups and cause membrane expansion, making the membrane less rigid, lowering the bending modulus and the tensile strength, and favoring a positive spontaneous curvature. Ethanol appears to have each of these characteristics but differs in terms of its interaction with the lipid headgroups. Ethanol is able to be involved in hydrogen bonding with various atoms of the

headgroups, including the carbonyl oxygens, whereas DMSO shows little or no involvement. As a result of this difference, the distribution of ethanol within the membrane is somewhat broader. The key difference between the formation of a water pore and an inverted micelle (or the intermediate structure characterizing hemifusion) is in the nature of the interfacial curvature; it is negative for ethanol-induced micelles and the hemifusion structure but positive for the DMSO-induced water pores. Although it is helpful to identify this core difference, the underlying cause(s) for this difference is not obvious. On the basis that both molecules cause undulations in the bilayer suggests they can support both negative and positive curvatures. It may be that the tensile strength/lipid desorption energy for ethanol is lower, which promotes desorption of lipids and micelle formation, whereas with DMSO the membrane is relatively more robust and attempts to retain some kind of contiguity about the pore structure.

An immediate and convenient inference from the simulation is that the inverse micelles serve to act as a delivery system, particularly for polar molecules including ions. Although we cannot observe the entire process of capture, transport, and delivery by the micelle structures within the simulations, the first two stages are indeed observed, occurring on a nanosecond time scale. Thus, ions are captured and end up within the
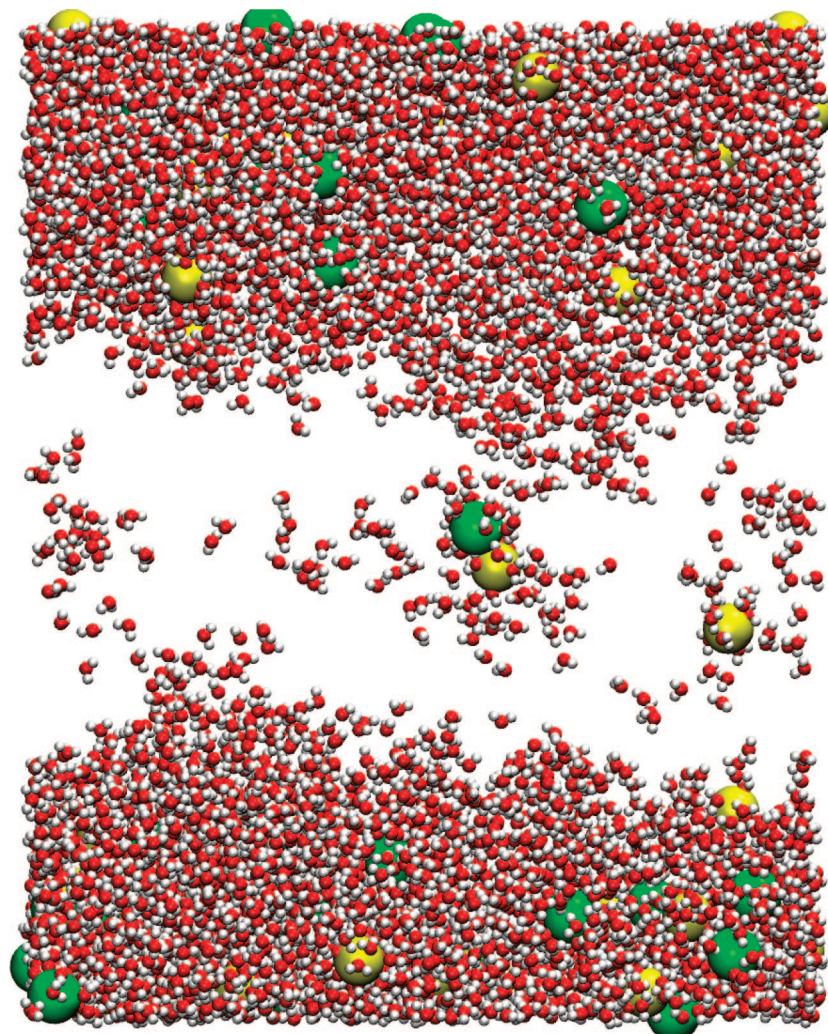
Figure 8. A POPC bilayer system in aqueous solution with 15 mol % of ethanol and 0.25 M of NaCl salt. Water is shown red and white, sodium ions in yellow, and chloride ions in green; ethanol molecules are not shown. For clarity, lipid molecules are not shown (white space in the middle of the snapshot). Presented is a structure after 53 400 ps of simulation.

membrane interior within 10−20 ns, whereas it would be virtually nigh impossible to observe an ion infiltrating an ethanol-free bilayer system over a period of microseconds of simulation.

As a final remark, ethanol-induced formation of non-bilayer structures within the membrane interior might have some relevance to pathological states caused by social consumption of alcohol. Although the typical concentration of ethanol in blood is 2 orders of magnitude lower than the threshold concentration of 12 mol % (30.5 v/v %) reported in this study, drinking strong alcoholic beverages such as vodka and whiskey would actually involve direct exposure of several epithelial tissues of the human body (lips, mouth, throat, gullet, and stomach) to high concentrations of ethanol (typically 40 v/v %, i.e. higher than the threshold concentration of 30.5 v/v %). These tissues are definitely much more robust compared to plasma membranes. However, ethanol-induced changes of the kind observed with associated consequences cannot fully be excluded.

Conclusion

We have performed extensive atomic-scale molecular dynamics simulations of phosphatidylcholine membranes in the Lα phase in aqueous solution with ethanol, with the objective of exploring the effects of ethanol as a function of its concentration. To this end, we systematically varied the ethanol concentrations in the range from 2.5 to 30 mol % (lipid-free basis).

At all concentrations at and below 12 mol %, ethanol is observed to cause marked membrane expansion with concomitant enhancement in interdigitation, which is in line with previous simulations and experiments. At concentrations of 12 mol % and above, ethanol causes desorption of the lipid molecules to form micelle-like structures containing water molecules within the bilayer interior. This observation is in line with laboratory experiments that revealed that the bilayer structure in a DPPC lipid system could not be maintained at high ethanol concentrations and formation of globular structures was observed.[42] Remarkably, we have observed that the threshold ethanol concentration at which the formation of non-bilayer structures is witnessed in the MD simulations closely matches the experimental value, namely 12 mol % (simulation) and 11.5 mol % (experiment).[42]

The phenomenon of micelle formation in the membrane interior appears to be generic, being reproducible in the simulations for both POPC and POPE bilayers. The non-bilayer structures are found to be relatively long-lived, and their formation is accompanied by mixing lipids that belong to the opposite membrane leaflets, thereby leading to irreversible

changes in the membrane structure. The micelle-like structures are also observed in simulations containing monovalent ions, with the ions being captured within the micelles. Therefore, the non-bilayer structures within the membrane interior have been shown to internalize water and ions and hence could serve as a delivery system for highly polar solutes and ions across membranes. Finally, we note that in all the (many) simulations of lipid bilayers with ethanol we did not observe the formation of any water pores.

References and Notes

(1) Littleton, J. M. *Biochem. Soc. Trans.* **1983**, *11* (1), 61–62.

(2) Williams, A. C.; Barry, B. W. *Adv. Drug Deliver. Rev.* **2004**, *56*, 603–618.

(3) Kurihara-Bergstrom, T.; Knutson, K.; De Noble, L. J.; Goates, C. Y. *Pharm. Res.* **1990**, *7*, 762–766.

(4) Mihic, S. J.; Ye, Q.; Wick, M. J.; Koltchine, V. V.; Krasowski, M. A.; Finn, S. E.; Mascia, M. P.; Valenzuela, C. F.; Hanson, K. K.; Greenblatt, E. P.; Harris, R. A.; Harrison, N. L. *Nature* **1992**, *389*, 385–389.

(5) Cantor, R. S. *Biochemistry* **1997**, *36*, 2339–2344.

(6) Holte, L. L.; Gawrisch, K. *Biochemistry* **1997**, *36*, 4669–4674.

(7) Feller, S. E.; Brown, C. A.; Nizza, D. T.; Gawrisch, K. *Biophys. J.* **2002**, *82*, 1396–1404.

(8) Barry, J. A.; Gawrisch, K. *Biochemistry* **1994**, *33*, 8082–8088.

(9) Vierl, U.; Lobbecke, L.; Nagel, N.; Cevc, G. *Biophys. J.* **1994**, *67*, 1067–1079.

(10) Ly, H. V.; Longo, M. L. *Langmuir* **2002**, *18*, 8988–8995.

(11) Ly, H. V.; Longo, M. L. *Biophys. J.* **2004**, *87*, 1013–1033.

(12) Patra, M.; Salonen, E.; Terama, E.; Vattulainen, I.; Faller, R.; Lee, B. W.; Holopainen, J.; Karttunen, M. *Biophys. J.* **2006**, *90*, 1121–1135.

(13) Chanda, J.; Bandyopadhyay, S. *Langmuir* **2006**, *22*, 3775–3781.

(14) Chanda, J.; Chakraborty, S.; Bandyopadhyay, S. *J. Phys. Chem. B* **2006**, *110*, 3791–3797.

(15) Terama, E.; Ollila, O. H. S.; Salonen, E.; Rowat, A. C.; Trandum, C.; Westh, P.; Patra, M.; Karttunen, M.; Vattulainen, I. *J. Phys. Chem. B* **2008**, *112*, 4131–4139.

(16) Dickey, A. N.; Faller, R. *Biophys. J.* **2007**, *92*, 2366–2376.

(17) Griepernau, B.; Leis, S.; Schneider, M. F.; Sikor, M.; Steppich, D.; Bockmann, R. A. *Biochim. Biophys. Acta* **2007**, *1768*, 2899–2913.

(18) Notman, R.; Noro, M.; O'Malley, B.; Anwar, J. *J. Am. Chem. Soc.* **2006**, *128*, 13982–13983.

(19) Gurtovenko, A. A.; Anwar, J. *J. Phys. Chem. B* **2007**, *111*, 10453–10460.

(20) Chanturiya, A.; Leikina, E.; Zimmerberg, J.; Chernomordik, L. V. *Biophys. J.* **1999**, *77*, 2035–2045.

(21) Berger, O.; Edholm, O.; Jahnig, F. *Biophys. J.* **1997**, *72*, 2002–2013.

(22) Berendsen, H. J. C.; Postma, J. P. M.; van Gunsteren, W. F.; Hermans, J. In *Intermolecular Forces*; Pullman, B., Ed.; Reidel: Dordrecht, 1981; pp 331−342.

(23) Lindahl, E.; Hess, B.; van der Spoel, D. *J. Mol. Model.* **2001**, *7*, 306–317.

(24) Darden, T.; York, D.; Pedersen, L. *J. Chem. Phys.* **1993**, *98*, 10089–10092.

(25) Essman, U.; Perera, L.; Berkowitz, M. L.; Darden, T.; Lee, H.; Pedersen, L. G. *J. Chem. Phys.* **1995**, *103*, 8577–8592.

(26) Berendsen, H. J. C.; Postma, J. P. M.; van Gunsteren, W. F.; DiNola, A.; Haak, J. R. *J. Chem. Phys.* **1984**, *81*, 3684–3690.

(27) Gurtovenko, A. A.; Vattulainen, I. *J. Am. Chem. Soc.* **2007**, *129*, 5358–5359.

(28) Gurtovenko, A. A.; Vattulainen, I. *J. Phys. Chem. B* **2008**, *112*, 1953–1962.

(29) Tieleman, D. P.; Berendsen, H. J. C. *Biophys. J.* **1998**, *74*, 2786–2801.

(30) Straatsma, T. P.; Berendsen, H. J. C. *J. Chem. Phys.* **1988**, *89*, 5876–5886.

(31) Beglov, D.; Roux, B. *J. Chem. Phys.* **1994**, *100*, 9050–9063.

(32) Hyslop, P. A.; Morel, B.; Sauerheber, R. D. *Biochemistry* **1990**, *29*, 1025–1038.

(33) Lantzsch, G.; Binder, H.; Heerklotz, H.; Wendling, M.; Klose, G. *Biophys. Chem.* **1996**, *58*, 289–302.

(34) Konig, B.; Dietrich, U.; Klose, G. *Langmuir* **1997**, *13*, 525–532.

(35) Smaby, J. M.; Momsen, M. M.; Brockman, H. L.; Brown, R. E. *Biophys. J.* **1997**, *73*, 1492–1505.

(36) Bockmann, R. A.; Hac, A.; Heimburg, T.; Grubmuller, H. *Biophys. J.* **2003**, *85*, 1647–1655.

(37) Mukhopadhyay, P.; Vogel, H. J.; Tieleman, D. P. *Biophys. J.* **2004**, *86*, 337–345.

(38) Leekumjorn, S.; Sum, A. K. *J. Phys. Chem. B* **2007**, *111*, 6026–6033.

(39) Lee, B. W.; Faller, R.; Sum, A. K.; Vattulainen, I.; Patra, M.; Karttunen, M. *Fluid Phase Equilib.* **2004**, *225*, 63–68.

(40) Chiu, S. W.; Clark, M.; Balaji, V.; Subramaniam, S.; Scott, H. L.; Jacobsson, E. *Biophys. J.* **1995**, *69*, 1230–1245.

(41) Hofsass, C.; Lindahl, E.; Edholm, O. *Biophys. J.* **2003**, *84*, 2192–2206.

(42) Mou, J.; Yang, J.; Huang, C.; Shao, Z. *Biochemistry* **1994**, *33*, 9981–9985.

(43) Gurtovenko, A. A.; Patra, M.; Karttunen, M.; Vattulainen, I. *Biophys. J.* **2004**, *86*, 3461–3472.

(44) McIntosh, T. J. *Chem. Phys. Lipids* **1996**, *81*, 117–131.

(45) Isomaa, B.; Hagerstrand, H.; Paatero, G. *Biochim. Biophys. Acta* **1987**, *899*, 93–103.

(46) Hornby, A. P.; Cullis, P. R. *Biochim. Biophys. Acta* **1981**, *647*, 285–292.

(47) Veiro, J. A.; Khalifah, R. G.; Rowe, E. S. *Biochim. Biophys. Acta* **1989**, *979*, 251–256.